quantum reports

CITESCORE 2.4

Article

A Study of Strong Confinement Regions Using Informational Entropy

Ademir de J. Santos, Frederico V. Prudente, Marcilio N. Guimarães and Wallas S. Nascimento

MDPI

https://doi.org/10.3390/quantum4040039

quantum reports

MDPI

Article

A Study of Strong Confinement Regions Using Informational Entropy

Ademir de J. Santos, Frederico V. Prudente *, Marcilio N. Guimarães and Wallas S. Nascimento

Instituto de Física, Universidade Federal da Bahia, Salvador 40170-115, Bahia, Brazil
* Correspondence: prudente@ufba.br

Abstract: We present an informational study of a spherically confined hydrogen atom, a hydrogenic ion confined in a strongly coupled plasma, a spherically confined harmonic oscillator, and a particle confined in a cage. For this, we have implemented a numerical procedure to obtain information entropies of these confined quantum systems. The procedure is based on the variational formalism that uses the finite element method (FEM) for the expansion of the wavefunction in terms of local base functions. Such a study is carried out in order to analyze what happens in the rigorous confinement regime. In particular, we have shown that the effects of the interaction potential is no longer important for rigorous confinements and the studied systems start to behave just like an electron confined by a impenetrable spherical cage. When possible, we compared our results with those published in the literature.

Keywords: Shannon entropy; confined quantum systems; finite element method

Citation: Santos, A.d.J.; Prudente, F.V.; Guimarães, M.N.; Nascimento, W.S. A Study of Strong Confinement Regions Using Informational Entropy. *Quantum Rep.* **2022**, *4*, 544–557. https://doi.org/10.3390/quantum4040039

Academic Editor: Carlo Cafaro

Received: 2 October 2022
Accepted: 19 November 2022
Published: 23 November 2022

1. Introduction

The study of confined quantum systems is a field that examines the spatial limitation effects on the physical properties of the electrons, nuclei, atoms, or molecules. The literature contains several theoretical and experimental works indicating that the spatial confinement changes the physical and chemical properties of the systems [1–3]. For instance, when the hydrogen atom is confined by impenetrable walls the energy spectrum is altered; moreover, in confined environments some alkali metals present electronic configurations similar to those of transition metals [4,5]. In recent years, with the increases in computational capacity and the development of modern techniques, this question has received considerable attention [6–10].

In the Schrödinger equation that describes the confined system, we can use a model potential that has both nuclear and confinement potential properties [11]. The choice of the potential model depends on the physical system of interest and of the characteristics of the confinement [12–16]. For instance, we can use infinite potential barriers models [17,18] or soft barriers models [19,20].

In particular, strong or rigorous confinement region includes interesting details such as: (a) it has a highly concentrated probability density when compared to the weakly confined regions; (b) the kinetic energy of electrons is large in contrast to their potential energy; and (c) the influence of the confinement barrier becomes greater than the free system potential [21–24]. The rigorous confinement region is established when the confinement radius of the system goes to zero. Energy studies based on ionization energy have been successfully undertaken in mapping this specific region [25–27].

In the atomic, molecular and chemical-physical context we define the informational entropies (or Shannon entropy) on position, S_r; on momentum, S_p; spaces; and the entropy sum, S_t, by adding S_r and S_p [28,29]. These informational quantities have been utilized in the study of various confined quantum systems such as the confined hydrogen-like atoms [30–35], the confined He-like atoms [36,37], plasma environments [38,39], and

in many other systems [40–42]. Analysis of basis functions [29,43] and electronic correlation [36,44,45], as well as physical and chemical phenomena [46–49] are also being approached in the informational field.

Despite of the energy analysis, the information entropies have been used as a powerful tool to study the regions where the effects of confinement are extreme. According to previous studies using entropic quantities, we have that the influence of the one-dimensional harmonic [50] and Coulomb [29] potentials is practically nullified by the presence of strong confinement. Moreover, in this specific region of the system (where the confinement radius tends to zero) the effects of Coulomb correlation in confined helium-like atoms become negligible [36].

The main goal of this work is to analyze how information entropy can contribute to the understanding of the strong confinement regime. For this, we have determined entropic quantities of interest for the spherically confined hydrogen atom, the hydrogenic ion confined in a strongly coupled plasma, and the spherically confined harmonic oscillator and compare them with the results of a particle confined in a cage.

This paper is organized as follows: in Section 2 we present the physical systems of interest, the numerical procedures based on the variational formalism using the finite element method, and beyond the informational formalism adopted; in Section 3 we discuss the results obtained; and, finally, in Section 4 we summarize the central aspects of our investigation.

2. Theoretical Background

In this section, we present the concepts and methods applied in our research. In Section 2.1, we discuss the physical systems and the variational formulation of the problem. Moreover, in Section 2.2, we define the informational quantities of interest.

2.1. System of Interest

The radial Schrödinger equation, using atomic units, is given by

$$\left[-\frac{1}{2r^2}\frac{d}{dr}r^2\frac{d}{dr}+\frac{l(l+1)}{2r^2}+V(r)-E_{nl}\right]\varphi_{nl}(r)=0\,, \tag{1}$$

where $\varphi_{nl}(r)$ is the radial wavefunction solution, E_{nl} the energy of the stationary state, and $V(r)$ the potential model. The labels n and l refer to the main and angular quantum numbers, respectively. The total wavefunction solution for a particular (n,l,m) quantum numbers is given by

$$\psi_{nlm}(\vec{r})=\varphi_{nl}(r)\;Y_{lm}(\Omega)\,, \tag{2}$$

where $Y_{lm}(\Omega)$ is the correspondent spherical harmonic and Ω is the solid angled.

Here, we consider four different model potentials of the type infinite spherical barrier to confine an electron. For models that contain an atomic nucleus, it is located at the center of the hard sphere. Our starting point is the potential that describes a particle (electron) confined in a spherical cage, that is,

$$V_1(r)=\begin{cases}0\,, & 0<r<r_c\\ \infty\,, & r\geq r_c\end{cases}\,, \tag{3}$$

where r_c is the confinement radius. For the r range of values between $0<r<r_c$ the particle is free of potential and at the confinement frontier the value of the potential is infinite.

Following, we have the Coulomb potential model of confined hydrogenic-like atoms,

$$V_2(r)=\begin{cases}-\frac{Z}{r}\,, & 0<r<r_c\\ \infty\,, & r\geq r_c\end{cases}\,, \tag{4}$$

where Z is the nuclear charge. We also consider an electron under influence of the isotropic harmonic potential, given by,

$$V_3(r) = \begin{cases} \frac{1}{2}\omega^2 r^2\,, & 0 < r < r_c \\ \infty\,, & r \geq r_c \end{cases}\,, \tag{5}$$

where ω is the angular frequency.

Finally, we selected to study one electron in a plasmatic environment of the sphere model. For strongly coupled plasma surrounding an ion having a single valence electron, one can define a sphere of radius r_c such that the plasma electrons with density γ is sufficient to neutralize $(Z-1)$ of central positive charge:

$$r_c = \left[\frac{Z-1}{4\pi\gamma/3}\right]^{\frac{1}{3}}\,.$$

Under this condition the interaction potential energy of the electron with an ion is

$$V_4(r) = \begin{cases} -\frac{Z}{r} + \frac{(Z-1)}{2r_c}\left[3 - \left(\frac{r}{r_c}\right)^2\right] & \text{and} \quad r < r_c \\ \infty & \text{and} \quad r \geq r_c \end{cases}\,. \tag{6}$$

To solve the radial Schrödinger Equation (1) with the potentials (3), (4), (5), or (6) by using the variational principle, for a given angular moment l, it corresponds to find the results that agree with the extreme condition of the energy functional, $\delta J_l[\chi_{nl}] = 0$, where the function $\chi_{nl}(r) = r\varphi_{nl}(r)$ must vanish at the origin and at the surface of a sphere of radius $r = r_c$ due to confinement (boundary conditions).

In variational context, the radial wavefunctions and energy eigenvalues are found by expanding the function χ_{nl} in terms of a finite basis set $\{f_j\}$, that is,

$$\chi_{nl}(r) = \sum_{j=1}^{p} c_j f_j(r), \tag{7}$$

where $\{c_j\}$ are the coefficients of the expansion. The efficiency of the numerical calculation depends on the choice of the finite basis set. The variational solutions are obtained by solving the generalized eigenvalue eigenvector problem

$$\mathbf{H}^l\mathbf{c} = E\mathbf{O}\mathbf{c}\,, \tag{8}$$

where $\mathbf{c}$ is the vector of the expansion coefficients $\{c_j\}$, being

$$\{\mathbf{H}^l\}_{ij} = \int_0^{r_c} dr\,\left\{\frac{1}{2}\frac{df_i^*(r)}{dr}\frac{df_j(r)}{dr} + f_i^*(r)V_l^{ef}(r)f_j(r)\right\} \tag{9}$$

and

$$\{\mathbf{O}\}_{ij} = \int_0^{r_c} dr\, f_i^*(r)f_j(r)\,, \tag{10}$$

where the effective potential is written as $V_l^{ef}(r) = V(r) + l(l+1)/2r^2$.

The variational methodology that we use to solve the problem is the p-version of the finite element method (p-FEM). In the radial case, the p-FEM consist of dividing the range of integration $[0, r_c]$ into N_e elements, being the i-th element defined in the range of r_{i-1} up to r_i with $r_0 = 0$ and $r_{N_e} = r_c$, and the radial wavefunction is expanded in local base functions $\{f_j^i\}$ satisfying the following property:

$$f_j^i(r) = 0 \;\text{ if } r \notin [r_{i-1}, r_i]\,, \tag{11}$$

where $f_j^i(r)$ is the j-th polynomial associated with i-th element and is its highest order given by the parameter k_i. Thus, considering the properties (11), the matrix representation of any local operator assumes a block tridiagonal form and the spatial confinement on the radial wavefunction can be imposed easily just removing the basis function $f_{k_i}^{N_e}(r)$ of the expansion. For more details, see references [11,51,52].

2.2. Shannon Informational Entropy

The Shannon information entropy in the atomic, molecular, and chemical physics context can be defined in terms of quantum-mechanical wavefunction. Therefore, information entropies on position, S_r, and momentum, S_p, spaces, in atomic units, are recognized as [29]

$$S_r = -\int d\vec{r}\, |\psi_{nlm}(\vec{r})|^2 \, \ln\Big[\, |\psi_{nlm}(\vec{r})|^2\Big] \tag{12}$$

and

$$S_p = -\int d\vec{p}\, |\widetilde{\psi}_{nlm}(\vec{p})|^2 \, \ln\Big[\, |\widetilde{\psi}_{nlm}(\vec{p})|^2\Big]\,, \tag{13}$$

where $\psi_{nlm}(\vec{r})$ and $\widetilde{\psi}_{nlm}(\vec{p})$ are the total position and momentum space wavefunction, respectively. Detailed discussions of the dimensionality of expressions (12) and (13) can be found in Refs. [29,53].

Using the variable separation method the wavefunctions can be written as

$$\psi_{nlm}(\vec{r}) = \varphi_{nl}(r)\, Y_{lm}(\Omega) \quad \text{and} \quad \widetilde{\psi}_{nlm}(\vec{p}) = \widetilde{\varphi}_{nl}(p)\, Y_{lm}(\Omega)\,, \tag{14}$$

where Y_{lm} are the spherical harmonics and Ω is the solid angled. Furthermore, the relationship between $\widetilde{\varphi}_{nl}(p)$ and $\varphi_{nl}(r)$ is given by [54]

$$\widetilde{\varphi}_{nl}(p) = \int_0^{r_c} r^2 j_l(pr)\varphi_{nl}(r)dr\,, \tag{15}$$

being j_l the spherical Bessel function. Employing the expressions (14) in Equations (12) and (13) we separate the S_r and S_p entropies into two parts, that is [55],

$$S_r = S_\varphi + S_\Omega \tag{16}$$

and

$$S_p = S_{\widetilde{\varphi}} + S_\Omega\,. \tag{17}$$

The radial parts S_φ and $S_{\widetilde{\varphi}}$ that depends on the potential function are

$$S_\varphi = -\int_0^{r_c} dr\, r^2 |\varphi_{nl}(r)|^2 \ln\Big[|\varphi_{nl}(r)|^2\Big]\,, \tag{18}$$

and

$$S_{\widetilde{\varphi}} = -\int_0^{\infty} dp\, p^2 |\widetilde{\varphi}_{nl}(p)|^2 \ln\Big[|\widetilde{\varphi}_{nl}(p)|^2\Big]\,. \tag{19}$$

The angular contribution known as angular entropy (common for S_r and S_p) is given by

$$S_\Omega = -\int_\Omega d\Omega\, |Y_{lm}(\Omega)|^2 \ln\Big[|Y_{lm}(\Omega)|^2\Big]\,. \tag{20}$$

The S_Ω quantity is independent of the potential and has a closed form determined by

$$S_\Omega = -\log\left(\frac{(2l+1)(l-m)!}{4\pi(l+m)!}\right) - \left(\frac{(2l+1)(l-m)!}{2(l+m)!}\right)\int_{-1}^{1}[P_l^m(t)]^2 ln[P_l^m(t)]^2 dt\,, \tag{21}$$

where P_l^m is the Legendre function.

The S_t quantity is obtained from entropy sum of $S_r + S_p$. From the entropy sum we can still derive the following entropy uncertainty relation:

$$\begin{aligned} S_t &= S_r + S_p \\ &= -\int_0^{r_c}\int_0^{\infty} dr\, dp\, r^2\, p^2\, |\varphi_{nl}(r)|^2\, |\widetilde{\varphi}_{nl}(p)|^2\, \ln\left(|\varphi_{nl}(r)|^2\, |\widetilde{\varphi}_{nl}(p)|^2\right) + 2\, S_\Omega \\ &\geq 3\,(1+\ln\pi)\,. \end{aligned} \tag{22}$$

This entropy uncertainty relationship is also known as the BBM inequality relation [56], which it is a common theorem for any quantum system. From expression (23) we can obtain Kennard's uncertainty relationship as discussed in Ref. [56].

3. Results and Discussions

This section presents the data obtained respective analysis of Shannon entropies, in atomic units, for a particle confined in a spherical cage (Equation (3)), the confined hydrogen atom (Equation (4) with $Z = 1$), spherically confined harmonic oscillator (Equation (5) with $\omega = 1$), and hydrogenic ion confined in a strongly coupled plasma (Equation (6) with $Z = 2$). For this, we have implemented the procedure based on the theory presented previously using the computer language Fortran. Unless stated otherwise, all curves were fitted with cubic spline interpolation utilizing the free application SciDAVis. Particularly, for the hydrogen atom, our computational implementation obtained values equivalent to accurate results existing in the literature [33].

The difference, ΔS_r, between the values of position space entropy of each of the three systems and that of the particle confined in a cage, calculated by Equation (16), as function of confinement radius, r_c, on a logarithmic scale, are shown in Figure 1a–c, for the confined hydrogen atom, the confined ion in a strongly coupled plasma, and the spherically confined harmonic oscillator, respectively. We plot all states with principal quantum numbers $1 \leq n \leq 5$ and $0 \leq l \leq 4$. The first observation is that for the three systems the quantities ΔS_r tend to zero when the confinement radius decreases, indicating that in a rigorous confinement regime the position entropy of the systems tends to behave like that of a particle confined in a cage. The second observation is that, in general, the more excited the state, the faster ΔS_r moves towards zero. This is in agreement with our intuition that since the more excited states are less influenced by the interaction potential, they tend more quickly towards the behavior of a particle in a spherical cage.

Particularly, it can be seen that the behavior of the entropy difference of the hydrogen confined and the ion-sphere are very similar. By zooming the graph in the region of small radii (Figure 1a,b), it is visible that the $1s$ state is less influenced by confinement when compared to the others states. In turn, by zooming in on the graph (Figure 1c), it can be seen that the values of the position space entropy difference of the harmonic oscillator tend to zero for larger values of r_c than the others systems.

It is also remarkable that some regions of r_c have states with positive entropy differences. This is counterintuitive since the position Shannon entropy indicates the delocalization of density. Considering that one of the systems has an attractive potential, our intuition is that the density of this system would always be less spread out than that of the particle in a cage. The states that present $\Delta S_r > 0$ are $2s$, $3s$, $4s$, $5s$, $3p$, $4p$, $5p$, and $5d$, for the confined hydrogen and the ion-sphere; and, in the case of the harmonic oscillator, the states $4d$ and $5f$ are added.

In Figure 2a–c are shown the difference, ΔS_p, between the values of momentum space entropy of each of the three systems and that of the particle confined in a spherical cage, calculated from Equation (17), as function of r_c on a logarithmic scale, for the confined hydrogen atom, the confined ion in a strongly coupled plasma and the spherically confined harmonic oscillator, respectively. We have displayed in Figure all states with principal quantum numbers $1 \leq n \leq 5$ and $0 \leq l \leq 4$. We observe similar behavior to that of position space entropy when the confinement radius tends to zero, decreasing its amplitude gradually to zero. This confirms that the interaction potential is no longer important

for rigorous confinements and the system starts to behave like an electron confined in a spherical cage.

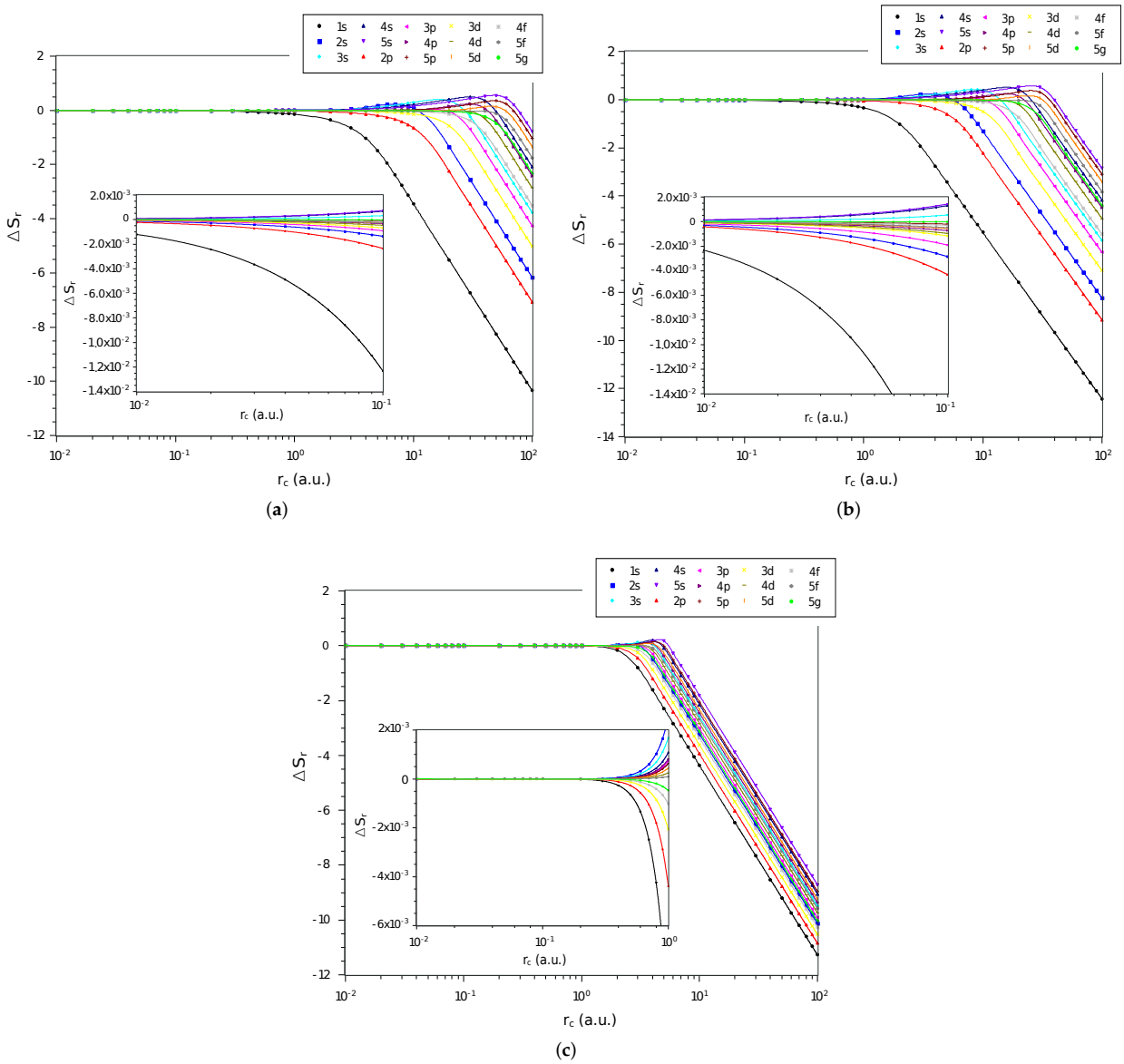

Figure 1. Values of ΔS_r in different quantum states as a function of r_c on a logarithmic scale for the (**a**) hydrogen confined, (**b**) ion-sphere, and (**c**) confined harmonic oscillator.

In the case of moment space entropy, the comparison between states and systems is quite similar to the one made for position space entropy. The sign change behavior of the entropy difference in some regions of r_c is also noticed for the hydrogen confined and the ion-sphere systems. In particular, the entropy difference of some states seems to oscillate more prominently when compared to the position space ones. The states that present $\Delta S_p < 0$ are $2s$, $3s$, $4s$, $5s$, $4p$, and $5p$ and $5d$, for the confined hydrogen and the ion-sphere, respectively; and, in the case of the harmonic oscillator, there are no regions with sign change.

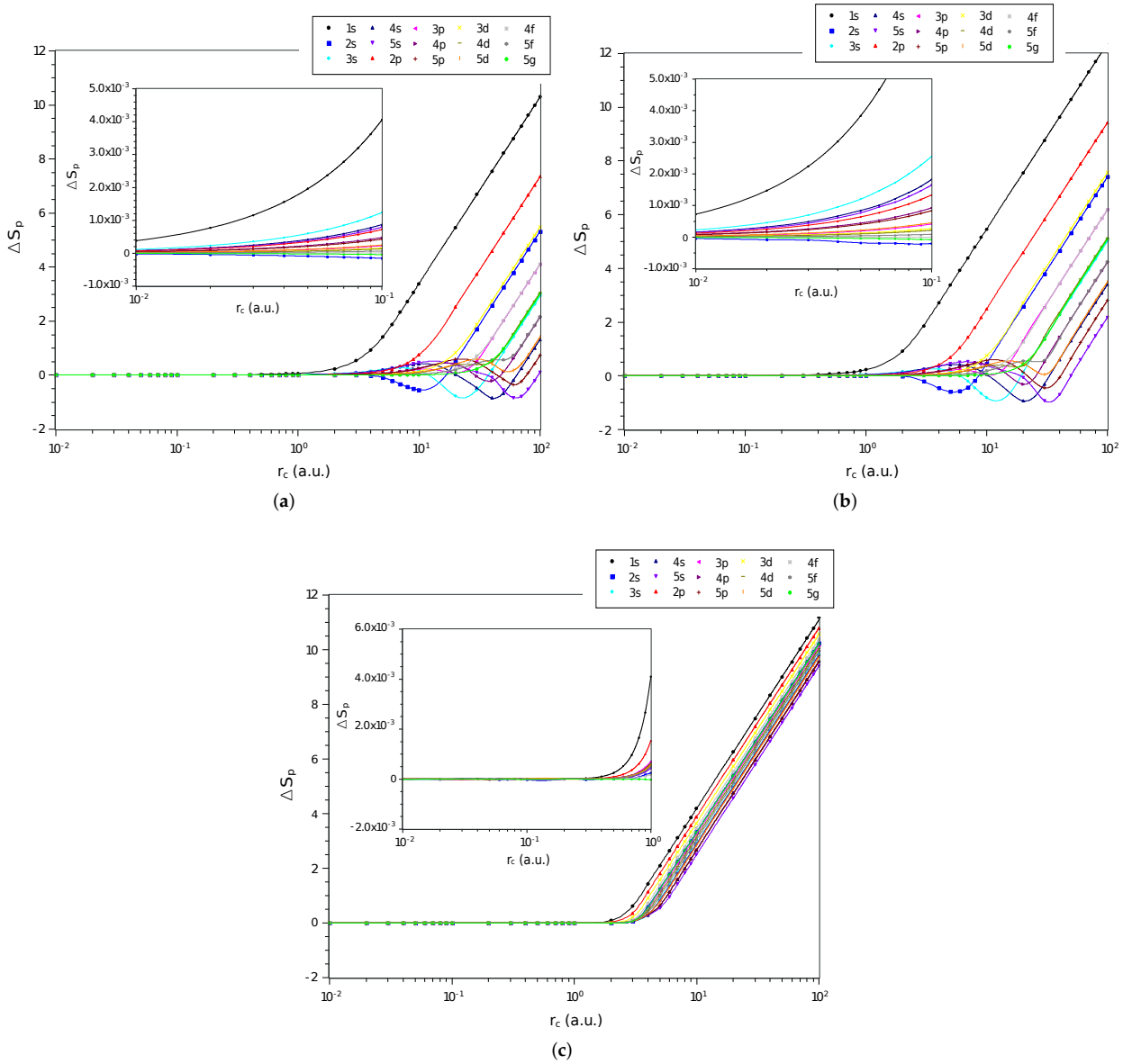

Figure 2. Values of ΔS_p in different quantum states as a function of r_c on a logarithmic scale for the (**a**) hydrogen confined, (**b**) ion-sphere, and (**c**) confined harmonic oscillator.

Now, we analyze the difference, ΔS_t, between the values of entropy sum of each of the three systems and that of the particle confined in a cage, calculated by Equation (23), as function of confinement radius, r_c. Specifically, ΔS_t for states with $1 \leq n \leq 5$ and $0 \leq l \leq 4$ are shown in Figure 3a–c for the confined hydrogen atom, the confined ion in a strongly coupled plasma and the spherically confined harmonic oscillator, respectively. Again we observe that all ΔS_t, for the three systems, tend to zero when the confinement radius decreases. This indicates that in a rigorous confinement regime the entropy sum tends to behave like that of a particle confined in a spherical cage.

However, a different behavior of ΔS_t can be noticed when compared with ΔS_r and ΔS_p for intermediate and large values of r_c. In the entropy sum case, the values of ΔS_t converge asymptotically to constant values. For the ΔS_r and ΔS_p quantities, the values increase (positively or negatively) due to the behavior of S_r and S_p for an electron confined in a spherical cage (see discussion at the end of this section).

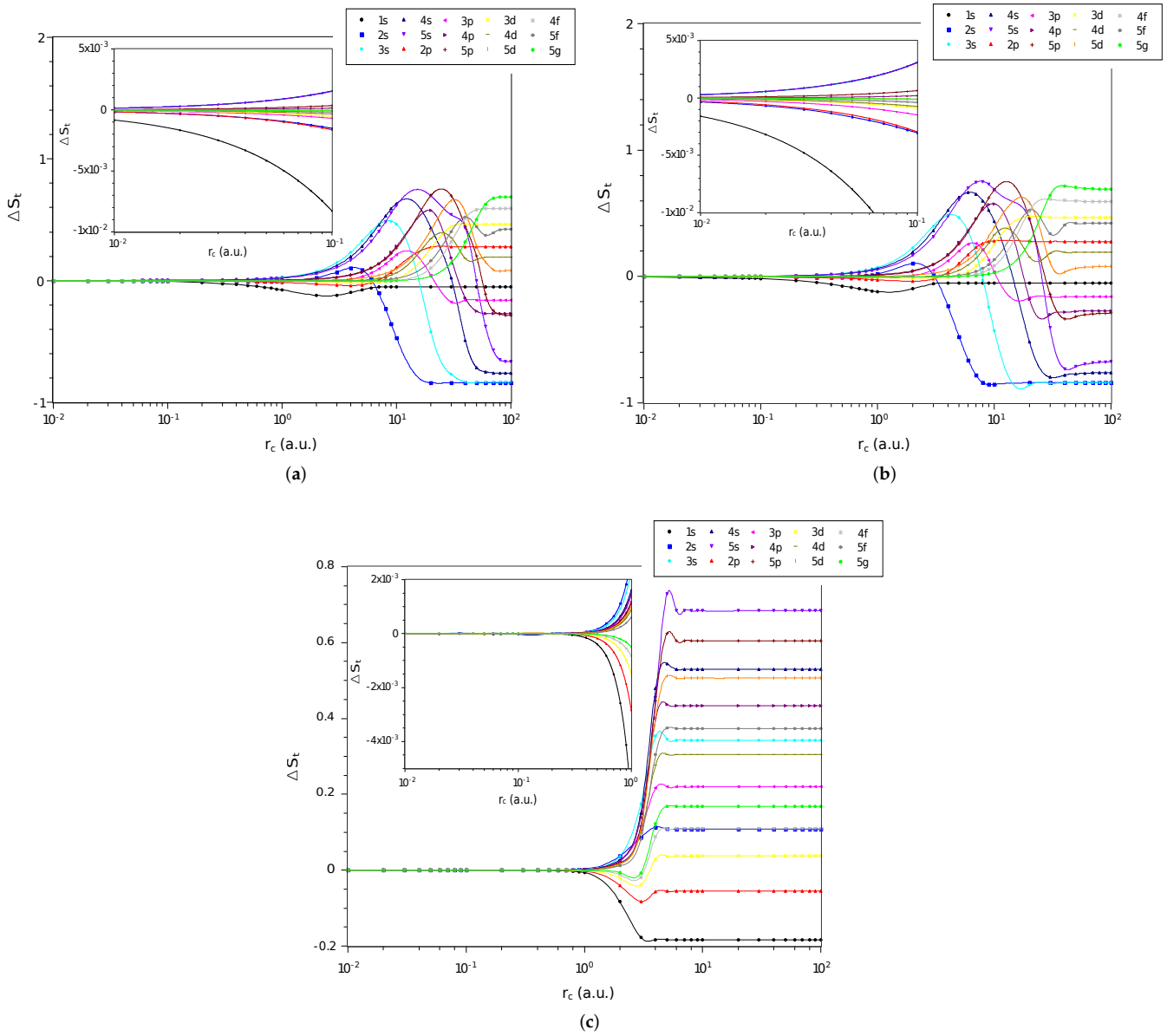

Figure 3. Values of ΔS_t in different quantum states as a function of r_c on a logarithmic scale for the (**a**) hydrogen confined, (**b**) ion-sphere, and (**c**) confined harmonic oscillator.

Note that a particular state of a given system with $\Delta S_t > 0$ ($\Delta S_t < 0$) has a larger (smaller) entropy sum than the same state for a particle confined in a cage for a given radius of confinement. That is, several states of the three systems under study have a lower entropy sum when free ($r_c >> 1$) than when subjected to strong confinement. For intermediate values of r_c we can observe oscillations in ΔS_t, confirming that confinement affects the position and momentum spaces differently.

The strong or rigorous confinement regime can be defined when the influence of the confining potential becomes greater than the free atomic system potential to specific configurations (or r_c values). Based on the entropy sum, S_t, of the ground state Nascimento et al. [36] defined three regions for confined atomic systems. The intermediate region is formed by r_c values that limit the half well depth in the ground state S_t versus r_c curve. The half well depth is given by

$$\sigma = \frac{S_t(r_c \to \infty) - S_t(r_c^{min})}{2}, \tag{23}$$

where S_t values are calculated in r_c tending to infinity and in r_c^{min} (r_c value where S_t assumes a minimal value). The strong and weak confinement correspond to the regions where are dominant the confinement ($r_c \to 0$) or Coulombian ($r_c \to \infty$) potentials, respectively. In Table 1, we determine the three regions from each of the three examined systems.

Table 1. Confinement regions for the hydrogen confined (HC), ion-sphere (IS), and confined harmonic oscillator (HO).

	σ	Strong	Intermediate	Weak
HC	0.040	$r_c < 1.17$	$1.17 \leq r_c \leq 4.51$	$r_c > 4.51$
IS	0.035	$r_c < 0.56$	$0.56 \leq r_c \leq 2.36$	$r_c > 2.36$
HO	0.000	$r_c < 2.00$ †	–	–

† Obtained from Figure 4.

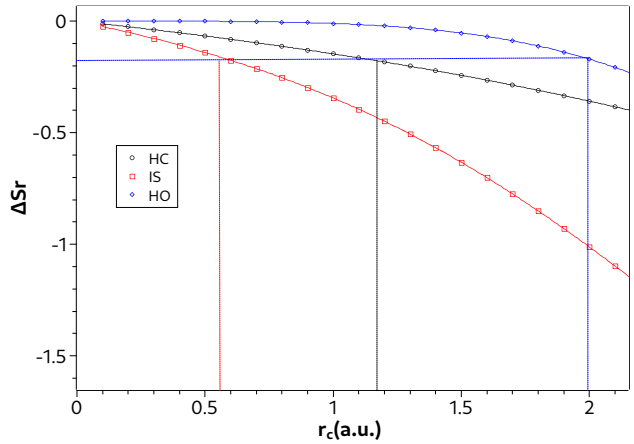

Figure 4. Values of ΔS_r in ground state as a function of r_c for the hydrogen confined (HC), ion-sphere (IS), and confined harmonic oscillator (HO). The vertical lines delimit the region of strong confinement for each system.

Note in Table 1 that the strong confinement region is smaller in the ion-sphere model than in the confined hydrogen atom. This indicates that, with respect to the confinement radius, the interaction potential of a hydrogen ion in a strongly coupled plasma surrounding is less influenced than the Coulomb potential of hydrogen atom. On the other hand, in the case of the harmonic oscillator, we verified that it was not possible to establish the three confinement regions by Equation (23), since there is no well in the ground state curve of S_t versus r_c. Indeed, as seen in Figure 3c, the influence of the confinement potential is greater even for larger confinement radii. To overcome this difficulty, we propose an additional criterion to deal with the harmonic oscillator case. To propose it, we consider Figure 4 where we show the values of ΔS_r in the ground state as a function of r_c for the three systems. In such a figure we notice that $\Delta S_r \approx -0.17$ in the confinement radius that defines the beginning of the strong confinement region for the hydrogenoid models. Thus, we propose the value of r_c when $\Delta S_r = -0.17$ to define the strong confinement region of the harmonic oscillator, written in Table 1. Establishing a criterion using S_r can be particularly advantageous in situations where it is difficult to calculate S_p.

Furthermore, in Figure 5a–d are shown the entropy sum, S_t, of the four systems as function of r_c on a logarithmic scale in the weak and intermediate regions ($1 \leq r_c \leq 100$). We plot all states with principal quantum numbers $1 \leq n \leq 4$ and $0 \leq l \leq 3$. Thus, it becomes clear from the figures for approximately which confinement radius, r_c, a given state of a specific system is in its lowest entropy sum configuration. Specifically, the $1s$ state is always the lowest entropy sum for all systems studied. On the other hand, some states have the lowest entropy sum for intermediate values of r_c, while others have a lower entropy for the free configuration or in the strong confinement region. Moreover, we see

that for the confined hydrogen atom and the ion confined in a strongly coupled plasma the states with angular momentum quantum number s (except the 1s state) are the most affected by confinement, while for the harmonic oscillator the 3s and 4s states, although affected, decrease their entropy sum.

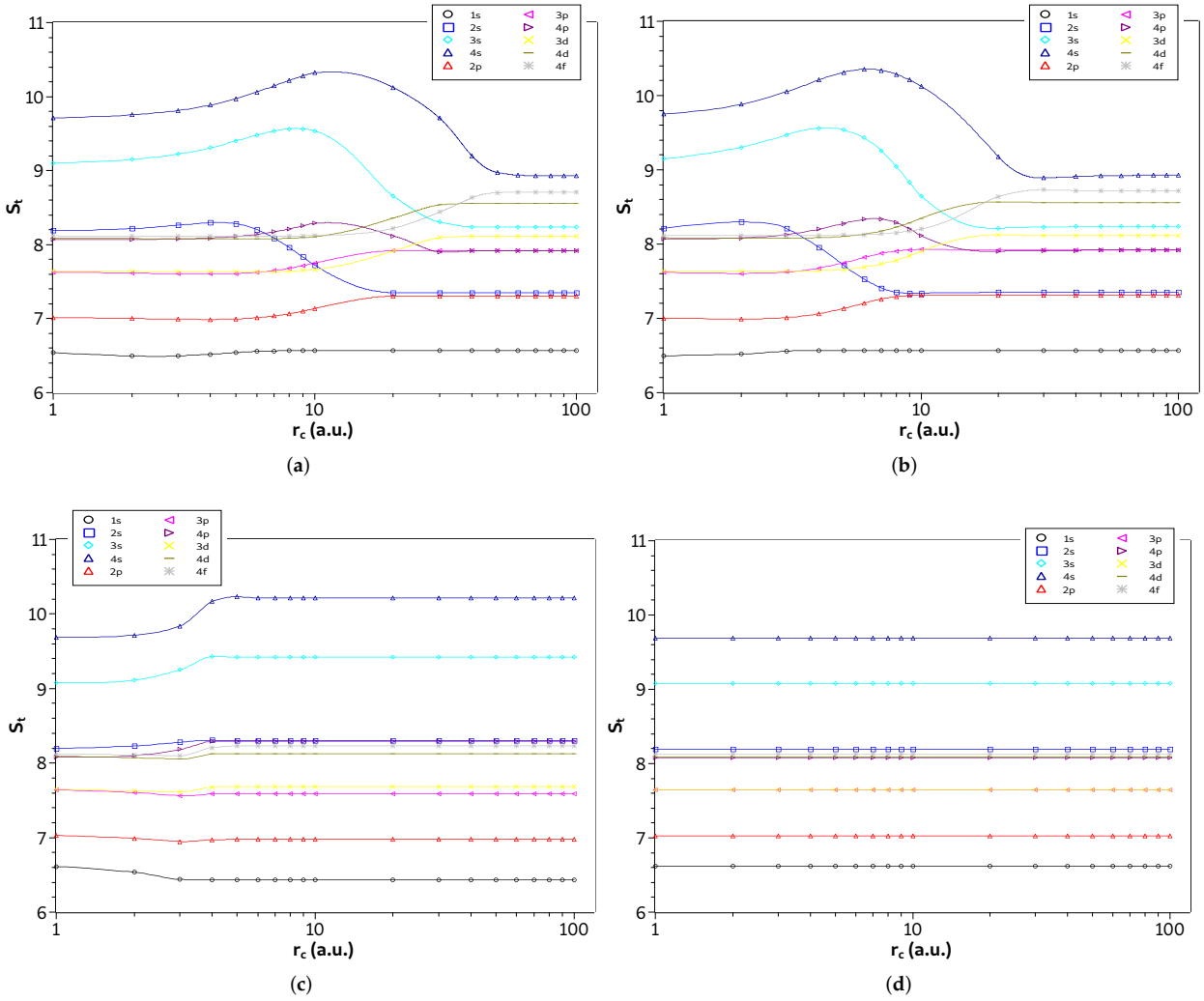

Figure 5. Values of S_t in different quantum states as a function of r_c on a logarithmic scale in the weak and intermediate regions for the (**a**) hydrogen confined, (**b**) ion-sphere, (**c**) confined harmonic oscillator, and (**d**) particle confined in a cage.

We now investigate only the particle confined in a spherical cage. In Figure 6, are displayed the entropies S_r and S_p as a function as a function of r_c on a logarithmic scale. We plot all states with principal quantum numbers $1 \leq n \leq 3$ and $0 \leq l \leq 2$. Note that the values of S_r are quite close for different quantum states. The same behavior was also observed by Nascimento et al. in [53] for the problem of one-dimensional infinite potential well. They have qualitatively explained such behavior by analyzing the probability densities in the position and momentum spaces. According to their explanation, the probability densities in the position are spread by same range of r values leading to equal values of S_r for all levels while in the momentum space the probability densities are spread for increasing ranges of p values leading to increase in S_p with the level increment.

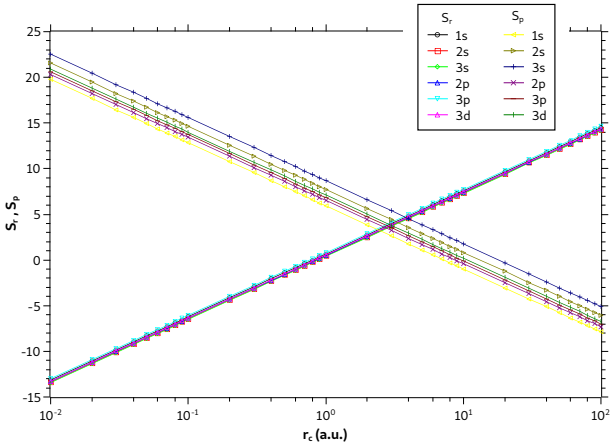

Figure 6. Values of S_r and S_p in different quantum states as a function of r_c on a logarithmic scale for the particle confined in a cage.

Moreover, Figure 6 also shows that entropies are linear on the monolog axes. In fact, the coefficient of determination gives $R^2 = 1$, demonstrating that the linear model fits perfectly to the sample of points. For the $1s$ state, for example, the linear regression fit of dataset gives $S_r = 3.0\log(r_c) + 0.7$ and $S_p = -3.0\log(r_c) + 5.9$; and for $2p$ state gives $S_r = 3.0\log(r_c) + 0.5$ and $S_p = -3.0\log(r_c) + 6.5$. As expected, the slopes of the straight lines S_r and S_p have opposite values so that in the sum $S_t = S_r + S_p$ the term with the $\log(r_c)$ will be canceled, showing that the entropy sum is constant, as it can be seen in Figure 5d. Note that the entropy curves for states $1s$ and $2p$ form two parallel lines (same slope) and that the S_r lines are much closer to each other (nearby y-intercepts) than the S_p lines.

Since it has been shown, in the strong confinement regime, that the three systems previously studied begin to behave like a particle confined in a spherical cage, then this also means that in this regime the entropies of these systems start to have a linear behavior as a function of $\log(r_c)$. Such behavior is evidenced by Figure 7, where we plot the graph of the values of entropy S_r in the ground state as a function of r_c on the logarithmic scale for the four systems in question. We can see in Figure 7 that the changes in behaviors for the linear trend of the confined particle happen almost abruptly near the regions of strong confinement defined in Table 1.

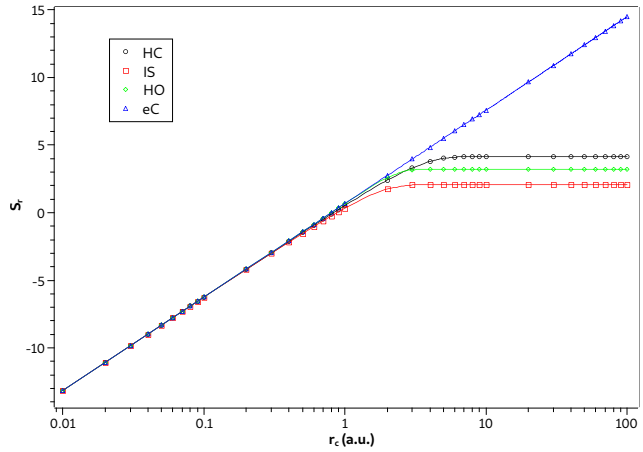

Figure 7. Values of S_r in ground state as a function of r_c on logarithmic scale for the hydrogen confined (HC), ion-sphere (IS), confined harmonic oscillator (HO), and particle confined (eC).

4. Conclusions

In this work, we presented a comparative study between some confined systems using Shannon's informational entropies as tools to analyze how the effects of confinement impact in these systems. For that, we implemented a computational code in Fortran based on the finite element method to solve the radial part of the Schorödinger equation. In particular, we determined the position and momentum space entropies and the entropy sum for different states of the following systems: a particle confined in a spherical cage, the spherically confined hydrogen atom, the hydrogenic ion confined in a strongly coupled plasma, and the spherically confined harmonic oscillator.

Our main observation was that the difference between values of entropies for all states of each of the three systems and that of the particle confined in a spherical cage tend to zero when the confinement radius decreases. This confirms that the interaction potential is no longer important for rigorous confinements and the system starts to behave just like an confined electron . Furthermore, we observed that the behavior of these entropies differences for the hydrogen confined and the ion-sphere are very similar, while for the harmonic oscillator they tend to zero faster. A counterintuitive behavior also noticed for the hydrogen confined and the ion-sphere systems was the sign change of the entropy difference on position and momentum spaces in some regions of confinement radius indicating that the density of these systems is more spread out than that of the particle in a cage.

We also determined in this work the three confinement regions of three of the examined systems using a procedure based on entropy sum proposed by Nascimento et al. [36]; and an additional criterion, using the entropy of space, was required to define the strong confinement region of the harmonic oscillator. Lastly, we only investigate the particle confined in a spherical cage. Besides the quite close values of entropy in the position space for different quantum states, we observed that entropies are linear on monolog axis. This means that in strong confinement regime the entropies of the other systems start to behave as a logarithmic function of the confinement radius.

As a final conclusion, with the employment of a very accurate numerical procedure, we have shown significant results on the behavior of strongly confined quantum systems and demonstrated the feasibility of using Shannon's informational entropies as a tool to analyze such behavior. As a perspective, we intend to extend the method to calculate Shannon's informational entropy for excited states of two-electron atoms and artificial atoms in the presence of external fields.

Author Contributions: All authors contributed equally to this work. All authors have read and agreed to the published version of the manuscript.

Funding: This research received no external funding.

Data Availability Statement: Data are available from the authors after a reasonable request.

Acknowledgments: We acknowledge the partial financial support provided by the Brazilian "Coordenação de Aperfeiçoamento de Pessoal de Nível Superior" (CAPES)—Finance Code 001. A.J.S. is grateful to "Conselho Nacional de Desenvolvimento Científico e Tecnológico" (CNPq) for grants. F.V.P. is also grateful for the provision of computational time in the Centro Nacional de Computação (CESUP), Universidade Federal do Rio Grande do Sul.

Conflicts of Interest: The authors declare no conflicts of interest.

References

1. Connerade, J.P. Confining and compressing the atom. *Eur. Phys. J. D* **2020**, *74*, 211. [CrossRef]
2. Sen, K.D. (Ed.) *Electronic Structure of Quantum Confined Atoms and Molecules*; Springer: Cham, Switzerland, 2014. [CrossRef]
3. Sabin, J.R.; Brändas, E.; Cruz, S.A. (Eds.) *Advances in Quantum Chemistry: Theory of Confined Quantum Systems vol 57 e 58*; Academic Press: New York, NY, USA, 2009.

4. García-Miranda, J.J.; Garza, J.; Ibarra, I.A.; Martínez, A.; Martínez-Sánchez, M.A.; Rivera-Almazo, M.; Vargas, R., Electronic Structure of Systems Confined by Several Spatial Restrictions. In *Chemical Reactivity in Confined Systems*; John Wiley Sons, Ltd.: Hoboken, NJ, USA, 2021; Chapter 4, p. 69. [CrossRef]
5. LEY-KOO, E. Recent progress in confined atoms and molecules: Superintegrability and symmetry breakings. *Rev. Mex. Fis.* **2018**, *64*, 326. [CrossRef]
6. El-Gammal, F.N. Confined atoms in plasma environment: variational Monte Carlo calculations. *Mol. Phys.* **2021**, *119*, e1879302. [CrossRef]
7. Maniero, A.M.; de Carvalho, C.R.; Prudente, F.V.; Jalbert, G. Oscillating properties of a two-electron quantum dot in the presence of a magnetic field. *J. Phys. B: At. Mol. Opt. Phys.* **2020**, *53*, 185001. [CrossRef]
8. Saha, S.; Jose, J. Shannon entropy as a predictor of avoided crossing in confined atoms. *Int. J. Quantum Chem.* **2020**, *120*, e26374. [CrossRef]
9. Cruz, E.; Aquino, N.; Prasad, V. Localization–delocalization of a particle in a quantum corral in presence of a constant magnetic field. *Eur. Phys. J. D* **2021**, *75*, 106. [CrossRef]
10. Deshmukh, P.C.; Jose, J.; Varma, H.R.; Manson, S.T. Electronic structure and dynamics of confined atoms. *Eur. Phys. J. D* **2021**, *75*, 166. [CrossRef]
11. Prudente, F.V.; Guimarães, M.N. Confined Quantum Systems Using the Finite Element and Discrete Variable Representation Methods. In *Electronic Structure of Quantum Confined Atoms and Molecules*; Sen, K.D., Ed.; Springer: Cham, Switzerland, 2014; Chapter 5, pp. 101–143.
12. Zicovich-Wilson, C.; Planelles, J.H.; Jaskólski, W. Spatially Confined Simple Quantum Mechanical Systems. *Int. J. Quantum Chem.* **1994**, *50*, 429. [CrossRef]
13. Costa, L.S.; Prudente, F.V.; Acioli, P.H.; Neto, J.J.S.; Vianna, J.D.M. A study of confined quantum systems using the Woods-Saxon potential. *J. Phys. B At. Mol. Opt. Phys.* **1999**, *32*, 2461. [CrossRef]
14. Connerade, J.P.; Dolmatov, V.K.; Lakshmi, P.A.; Manson, S.T. Electron structure of endohedrally confined atoms: Atomic hydrogen in an attractive shell. *J. Phys. B At. Mol. Opt. Phys.* **1999**, *32*, L239. [CrossRef]
15. Baltenkov, A.S. Resonances in photoionization cross sections of inner subshells of atoms inside the fullerene cage. *J. Phys. B: At. Mol. Opt. Phys.* **1999**, *32*, 2745. [CrossRef]
16. Nascimento, E.M.; Prudente, F.V.; Guimarães, M.N.; Maniero, A.M. A study of the electron structure of endohedrally confined atoms using a model potential. *J. Phys. B At. Mol. Opt. Phys.* **2011**, *44*, 015003. [CrossRef]
17. Salazar, S.J.C.; Laguna, H.G.; Prasad, V.; Sagar, R.P. Shannon-information entropy sum in the confined hydrogenic atom. *Int. J. Quantum Chem.* **2020**, *120*, e26188. [CrossRef]
18. d. S. T de Morais, G.; Custodio, R. Assessment of a numeric variational method for the solution of confined multielectron atoms. *J. Mol. Model.* **2021**, *27*, 212. [CrossRef]
19. Rodriguez-Bautista, M.; Vargas, R.; Aquino, N.; Garza, J. Electron-density delocalization in many-electron atoms confined by penetrable walls: A Hartree–Fock study. *Int. J. Quantum Chem.* **2018**, *118*, e25571. [CrossRef]
20. Pasteka, L.F.; Helgaker, T.; Saue, T.; Sundholm, D.; Werner, H.J.; Hasanbulli, M.; Major, J.; Schwerdtfeger, P. Atoms and molecules in soft confinement potentials. *Mol. Phys.* **2020**, *118*, e1730989.' [CrossRef]
21. Barbosa, T.N.; Almeida, M.M.; Prudente, F.V. A quantum monte carlo study of confined quantum systems: Application to harmonic oscillator and hydrogenic-like atoms. *J. Phys. B At. Mol. Opt. Phys.* **2015**, *48*, 055002. [CrossRef]
22. Prudente, F.V.; Costa, L.S.; Viana, J.D.M. A study of two-electron quantum dot spectrum using discrete variable representation method. *J. Chem. Phys.* **2005**, *123*, 224701. [CrossRef]
23. Bielinska-Waz, D.; Karwowski, J.; Diercksen, G.H.F. Spectra of confined two-electron atoms. *J. Phys. B At. Mol. Opt. Phys.* **2001**, *34*, 1987. [CrossRef]
24. Gueorguiev, V.G.; Rau, A.R.P.; Draayer, J.P. Confined one-dimensional harmonic oscillator as a two-mode system. *Am. J. Phys.* **2006**, *74*, 394. [CrossRef]
25. Montgomery, H.; Aquino, N.; Flores-Riveros, A. The ground state energy of a helium atom under strong confinement. *Phys. Lett. A* **2010**, *374*, 2044. [CrossRef]
26. Aquino, N.; Flores-Riveros, A.; Rivas-Silva, J. The compressed helium atom variationally treated via a correlated Hylleraas wave function. *Phys. Lett. A* **2003**, *307*, 326. [CrossRef]
27. Flores-Riveros, A.; Aquino, N.; Montgomery, H. Spherically compressed helium atom described by perturbative and variational methods. *Phys. Lett. A* **2010**, *374*, 1246. [CrossRef]
28. Sen, K.D., Ed. *Statistical Complexity: Applications in Electronic Struture*; Springer: Dordrecht, The Netherlands, 2011. [CrossRef]
29. Nascimento, W.S.; Prudente, F.V. Shannon entropy: A study of confined hydrogenic-like atoms. *Chem. Phys. Lett.* **2018**, *691*, 401. [CrossRef]
30. Estañón, C.R.; Aquino, N.; Puertas-Centeno, D.; Dehesa, J.S. Crámer-Rao complexity of the confined two-dimensional hydrogen. *Int. J. Quantum Chem.* **2021**, *121*, e26424. [CrossRef]
31. Mukherjee, N.; Roy, A.K. Information-entropic measures for non-zero l states of confined hydrogen-like ions. *Eur. Phys. J. D* **2018**, *72*, 118. [CrossRef]
32. Majumdar, S.; Mukherjee, N.; Roy, A.K. Various complexity measures in confined hydrogen atom. *Chem. Phys. Lett.* **2017**, *687*, 322. [CrossRef]

33. Jiao, L.; Zan, L.; Zhang, Y.; Ho, Y. Benchmark values of Shannon entropy for spherically confined hydrogen atom. *Int. J. Quantum Chem.* **2017**, *117*, e25375. [CrossRef]
34. Martínez-Flores, C. Shannon entropy and Fisher information for endohedral confined one- and two-electron atoms. *Phys. Lett. A* **2021**, *386*, 126988. [CrossRef]
35. Martínez-Sánchez, M.A.; Vargas, R.; Garza, J. Shannon Entropy for the Hydrogen Atom Confined by Four Different Potentials. *Quantum Rep.* **2019**, *1*, 208. [CrossRef]
36. Nascimento, W.S.; de Almeida, M.M.; Prudente, F.V. Coulomb Correlation and Information Entropies in Confined Helium-Like Atoms. *Eur. Phys. J. D* **2021**, *75*, 171. [CrossRef]
37. Majumdar, S.; Roy, A.K. Shannon Entropy in Confined He-Like Ions within a Density Functional Formalism. *Quantum Rep.* **2020**, *2*, 189. [CrossRef]
38. Lee, M.J.; Jung, Y.D. Characteristics of Shannon's Information Entropy of Atomic States in Strongly Coupled Plasma. *Entropy* **2020**, *22*. [CrossRef]
39. Zan, L.R.; Jiao, L.G.; Ma, J.; Ho, Y.K. Information-theoretic measures of hydrogen-like ions in weakly coupled Debye plasmas. *Phys. Plasmas* **2017**, *24*, 122101. [CrossRef]
40. Carrillo, R.S.; Gil-Barrera, C.A.; Sun, G.H.; Solaimani, M.; Dong, S.H. Shannon entropies of asymmetric multiple quantum well systems with a constant total length. *Eur. Phys. J. Plus* **2021**, *136*, 1060. [CrossRef]
41. Carrillo, R.S.; Dong, Q.; Sun, G.H.; Silva-Ortigoza, R.; Dong, S.H. Shannon entropy of asymmetric rectangular multiple well with unequal width barrier. *Results Phys.* **2022**, *33*, 105109. [CrossRef]
42. Song, X.D.; Sun, G.H.; Dong, S.H. Shannon information entropy for an infinite circular well. *Phys. Lett. A* **2015**, *379*, 1402. [CrossRef]
43. Gadre, S.R.; Sears, S.B.; Chakravorty, S.J.; Bendale, R.D. Some novel characteristics of atomic information entropies. *Phys. Rev. A* **1985**, *32*, 2602. [CrossRef]
44. Site, L.D. Shannon entropy and many-electron correlations: Theoretical concepts, numerical results, and Collins conjecture. *Int. J. Quantum Chem.* **2014**, *115*, 1396. [CrossRef]
45. Saha, S.; Jose, J. Shannon entropy as an indicator of correlation and relativistic effects in confined atoms. *Phys. Rev. A* **2020**, *102*, 052824. [CrossRef]
46. Sabirov, D.S.; Osawa, E. Information Entropy of Fullerenes. *J. Chem. Inf. Model.* **2015**, *55*, 1576. [CrossRef] [PubMed]
47. Sabirov, D.S. Information entropy of mixing molecules and its application to molecular ensembles and chemical reactions. *Comput. Theor. Chem.* **2020**, *1187*, 112933. [CrossRef]
48. Sabirov, D.S. Information entropy changes in chemical reactions. *Comput. Theor. Chem.* **2018**, *1123*, 169. [CrossRef]
49. Park, K.; Kim, J.; Moon, S.; An, K. Maximal Shannon entropy in the vicinity of an exceptional point in an open microcavity. *Sci. Rep.* **2020**, *10*, 12551. [CrossRef]
50. Nascimento, W.S.; Prudente, F.V. Sobre um estudo da entropia de Shannon no contexto da mecânica quântica: Uma aplicação ao oscilador harmônico livre e confinado. *Quim. Nova* **2016**, *39*, 757. [CrossRef]
51. Guimarães, M.N.; Prudente, F.V. A study of the confined hydrogen atom using the finite element method. *J. Phys. B At. Mol. Phys.* 2005, *38*, 2811. [CrossRef]
52. Prudente, F.V.; Soares Neto, J.J. Optimized mesh for the finite-element method using a quantum-mechanical procedure. *Chem. Phys. Lett.* **1999**, *302*, 43. [CrossRef]
53. Nascimento, W.S.; de Almeida, M.M.; Prudente, F.V. Information and quantum theories: An analysis in one-dimensional systems. *Eur. J. Phys.* **2020**, *41*, 025405. [CrossRef]
54. Goldman, S.; Joslin, C. Spectroscopic properties of an isotropically compressed hydrogen atom. *J. Phys. Chem.* **1992**, *96*, 6021. [CrossRef]
55. Yáñez, R.J.; Van Assche, W.; González-Férez, R.; Dehesa, J.S. Entropic integrals of hyperspherical harmonics and spatial entropy of D-dimensional central potentials. *J. Math. Phys.* **1999**, *40*, 5675. [CrossRef]
56. Bialynicki-Birula, I.; Mycielski, J. Uncertainty relations for information entropy in wave mechanics. *Commun. Math. Phys.* **1975**, *44*, 129. [CrossRef]